

## Optical determination of the twist elastic constant of a smectic- $C^*$ liquid crystal

Fuzi Yang, G. W. Bradberry, and J. R. Sambles

*Thin Film and Interface Group, Department of Physics, University of Exeter, Exeter EX4 4QL, Devon, United Kingdom*

(Received 26 May 1995)

Optical excitation of half-leaky guided modes has been used to characterize in detail the optical tensor profile in a homeotropically aligned ferroelectric liquid crystal layer. Uniform homeotropic alignment is achieved with no surface aligning layer, by the application of an in-plane dc electric field when the liquid crystal is in the  $S_C^*$  phase. This gives rise to a monodomain ideal for optical characterization. Angle dependent reflectivity data are then taken for various applied in-plane fields, slowly allowing the helix of the  $S_C^*$  phase to rewind. Fitting the data to modeling theory yields the director profile in the cell that allows a determination, from a knowledge of the spontaneous polarization  $P_S$ , of the twist elastic constant  $B_3$ . With the assumption that the surface anchoring forces are weak, in effect negligible, these results provide the value of  $B_3$  for the effectively infinite, unconstrained material.

PACS number(s): 61.30.Gd, 61.30.Eb

### I. INTRODUCTION

Since the discovery of ferroelectricity in the  $S_C^*$  liquid crystals by Meyer *et al.* [1], ferroelectric  $S_C^*$  liquid crystals (FLC's) have received substantial attention principally because of their potential application in high speed optical switches and displays. Elastic constants are important in designing devices from  $S_C^*$  materials, although only a limited amount of experimental work has been undertaken to determine them [2–8]. This may be because theoretical problems involved in modeling the helical structures are substantial, particularly in homogeneously aligned cells. Not surprisingly, experimental attention has focused mainly on the homogeneously aligned state since bistable switching was demonstrated in such a surface stabilized FLC by Clark and Lagerwall [9]. The homeotropic cell, with its rather less constrained structure, has received little attention, yet it may provide far better opportunities for determining the director configuration and hence the elastic constants in an arrangement approximating more closely “free” material.

By using the selective reflection technique with a homeotropically aligned FLC cell, the helical pitch  $p$  can be determined [10–12]. Then by measuring the pitch variation under the application of an in-plane field normal to the helical axis, the twist elastic constant  $B_3$  of the FLC may be quantified [6,7,10]. It should be appreciated, however, that although the helical pitch of the homeotropically aligned FLC may give rise to strong Bragg reflection and thereby allow pitch determination, there are several problems with this technique.

First, with light incident normally on the homeotropically aligned cell surface, and the helical axis of the FLC along this incidence direction, in general only the first-order Bragg reflection may occur [7,10,11]. This in practice means that only short pitch FLCs ( $\leq 2 \mu\text{m}$  pitch) may be readily measured by using conventional visible and near infrared sources. Modifications to this simple technique using applied fields [7] or oblique incidence [12] still do not help with longer pitch materials. A

second problem with the selective reflection technique is that it is the optical pitch  $n_{av}p$  that is determined [11]. To obtain the real pitch  $p$ , the average refractive index  $n_{av}$  also has to be established [13]. This is not very satisfactory, since the analytic formula used to give  $n_{av}$  is a rather crude approximation, while a full and accurate treatment of the situation demands rather more elaborate experimentation. Third, even if the approximation for  $n_{av}$  is used to determine  $p$ , the cone angle of the FLC, the ordinary index, and the extraordinary index (assuming incorrectly uniaxiality) have still to be measured by some other procedure [7,10–13]. Often, measurements taken to quantify these numbers are from cells in which further assumptions have to be made about director alignments and in which voltages have been applied to cause a relatively simple director structure. Not too surprisingly, such measurements add further levels of uncertainty in quantifying the helical properties of these materials. A fourth problem with the selective reflection technique is that it is difficult to measure these reflections near  $T_C$  (the  $S_A$  to  $S_C^*$  phase transition temperature) because the reflectances near  $T_C$  are very weak [7]. So, in general, data are acquired at temperatures well removed from  $T_C$ . Finally, and a little less severely, the optical pitch measurement using selective reflection is often based on the assumption that the helical axis is perpendicular to the cell walls. This is unlikely to be true. There is strong evidence to suggest that the smectic layers generally tilt with respect to the wall normal [14].

Thus it would be of substantial benefit in the determination of FLC pitches to find a technique that allows the unambiguous measurements of this parameter. It would also, of course, be advantageous to have a technique that works for longer pitch materials ( $p \geq 2 \mu\text{m}$ ) and also has the potential for measurements near to  $T_C$  so that the behavior of the  $S_C^*$  material near to  $T_C$  may be established.

Recently, an extremely powerful optical technique for determining the director profile of a liquid crystal in a thin cell, the half-leaky guided mode (HLGM) technique,

has been reported [15,16]. Theoretical analysis and experimental data indicate that the  $s$  (transverse electric) to  $p$  (transverse magnetic) polarization conversion signals, in reflection with such a HLGGM geometry, over a narrow window of angles, is exquisitely sensitive to details of the director profile in the cell. Careful fits, using multilayer optics modeling theory, to angle dependent polarization conversion reflectivity for the HLGGM geometry allow the twist and tilt profile, the cell thickness, and the optical tensor to be quantified. Thus, in principle, a study of a homeotropically aligned FLC using this HLGGM technique should yield the tilt (cone angle) of the primary director axis and the form of the twist profile and therefore the pitch throughout the cell.

In the study presented here, it is just such a HLGGM procedure that has been applied to a cell containing homeotropically aligned FLC (Merck, SCE13). To ensure that surface anchoring has only a small effect on the director profile, measurements of the homeotropic alignment have been achieved using in-plane fields with no surface aligning layers. The cell walls are bare glass, on one of which are silver electrodes some 3 mm apart. It is between these two electrodes that the in-plane aligning field is applied.

As well as allowing the establishment of a mono-domain for study, the in-plane voltage may be slowly reduced so that the helical pitch progressively reestablishes itself. By quantifying how this happens as a function of voltage and through knowledge of the spontaneous polarization  $P_S$ , we obtain not only the pitch of the  $S_C^*$  material but also the twist elastic constant  $B_3$ . Because, as the voltage is reduced to zero, the system approximates closely that of free material, with the weak surface anchoring forces influencing only a thin boundary region, this allows the determination of the unconstrained pitch and  $B_3$  for this material.

## II. PRINCIPLES

The Cartesian coordinate system used throughout this study is shown in Fig. 1, with the  $z$  axis taken to be along the helical axis of the  $S_C^*$  material. This axis is for the moment assumed to be normal to the surfaces of the cell. In Fig. 1,  $\mathbf{n}$  is a unit vector parallel to the primary director of the FLC, where  $\mathbf{c}$  is a unit vector parallel to the projection of  $\mathbf{n}$  onto the smectic layer plane  $XOY$ . The tilt angle  $\theta$  is the angle between  $\mathbf{n}$  and the layer normal ( $z$  axis), and the twist or azimuthal angle  $\phi$  is the angle between  $\mathbf{c}$  and the  $x$  axis. A dc electric field  $E$  is applied along the  $y$  axis. The spontaneous polarization of the FLC,  $P_S$ , is in the smectic layer plane and perpendicular to both  $\mathbf{n}$  and  $\mathbf{c}$ . Note that for all material tensor properties the  $P_S$  axis is one of the diagonalization axes. If the system is treated as biaxial, then the two other diagonalization axes will be in the plane perpendicular to  $\mathbf{P}_S$  containing both  $\mathbf{n}$  and  $\mathbf{c}$ , but no axis need be parallel to  $\mathbf{n}$ . Only if we assume uniaxiality is  $\mathbf{n}$  strictly one of the tensor diagonalization axes. However, a reasonable approximation is to assume that this is very nearly the case.

When the bending and compression of the smectic layers are assumed to be negligible, then the variation of the

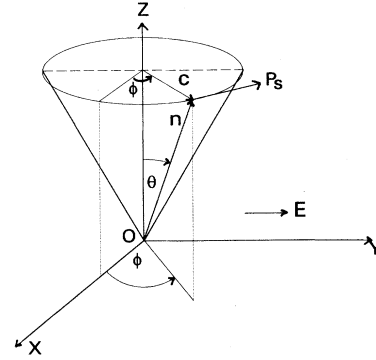


FIG. 1. Cartesian coordinate system used with  $z$  axis along the helical axis of the  $S_C^*$  material.

free energy with  $\phi$ , with an applied electric field along the  $y$  axis, may be cast in much the same form as that for cholesterics in the following manner [17–19]:

$$F(E) - F(E=0) = \int \left[ \frac{B_3}{2} \left( \frac{d\phi}{dz} - q_0 \right)^2 + \frac{\epsilon_a}{8\pi} \sin^2\theta \cos^2\phi E^2 - P_S E \cos\phi \right] dz, \quad (1)$$

where  $B_3$  is the twist elastic constant,  $q_0 = 2\pi/p_0$  ( $p_0$  is the helical pitch in the absence of a field),  $P_S = |\mathbf{P}_S|$ ,  $E = |\mathbf{E}|$ , and  $\epsilon_a = (\epsilon_{\parallel} - \epsilon_{\perp})$  is the dielectric anisotropy assuming uniaxiality. This equation may be much simplified by supposing the  $\mathbf{P}_S$  coupling term to be much stronger than the dielectric anisotropy term. Of course in the limit  $E \rightarrow 0$ , this has to be true. In the experiments

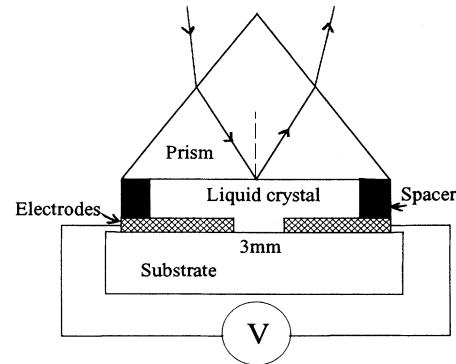


FIG. 2. Experimental arrangement used with high index prism ( $n = 1.800$ ), Mylar spacers (giving a spacer thickness of  $3.5 \mu\text{m}$ ), silver electrodes (spaced 3 mm apart), and a low index ( $n = 1.458$ ) substrate.

reported here,  $E$  is always less than  $5 \times 10^5 \text{ Vm}^{-1}$ , and it is only at high temperatures, close to the phase transition, that the  $\epsilon_a E^2$  term may become significant by comparison with the  $P_S E$  term, but then  $\theta \rightarrow 0$  also. Further, at all temperatures we shall explore the behavior of the cell as  $E$  tends to zero, where again the  $P_S E$  term is dominant. Thus we may simplify Eq. (1) by removing the  $\epsilon_a E^2$  term. This means the Euler-Lagrange equation governing the twist deformation in an applied dc field is

$$\frac{d^2 \phi}{dz^2} = \frac{P_S}{B_3} E \sin \phi. \quad (2)$$

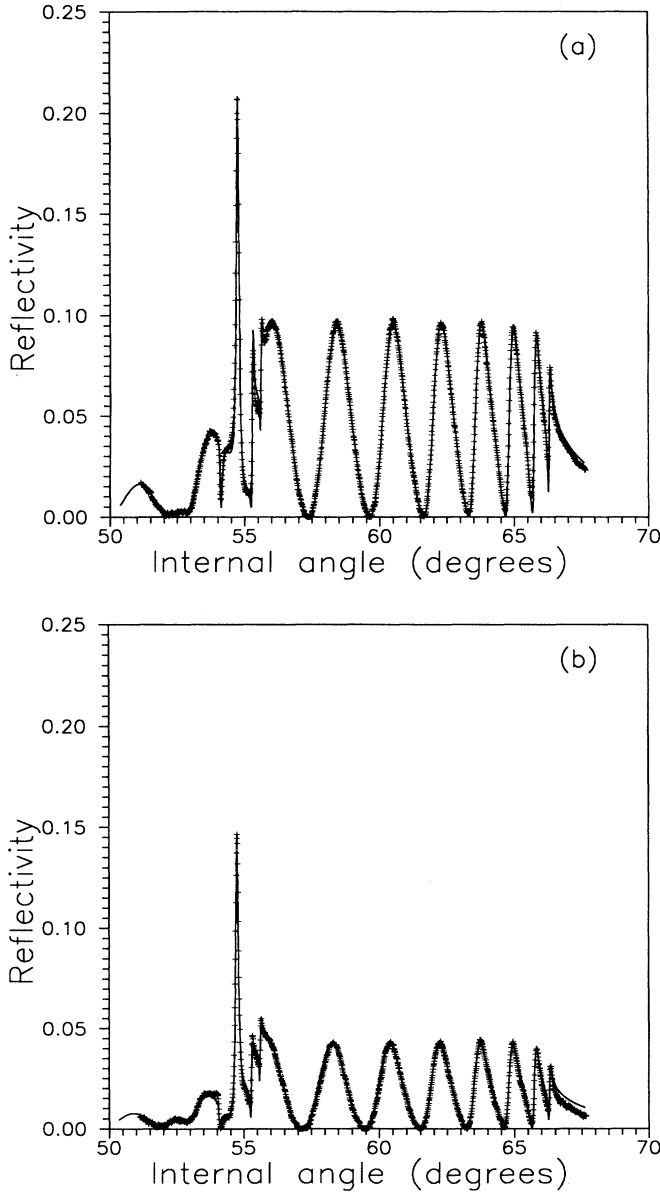


FIG. 3. Experimental data for the angular dependence of the  $s$  to  $p$  conversion reflectivity for the  $S_C^*$  phase at  $52.5^\circ\text{C}$  ( $\lambda = 632.8 \text{ nm}$ ) with (a)  $-1.5 \text{ kV}$  and (b)  $+1.5 \text{ kV}$  applied across the  $3 \text{ mm}$  gap. The solid lines show the result of theoretical modeling with  $\epsilon_1 = 3.2400$  and  $\epsilon_3 = 2.1240$ .

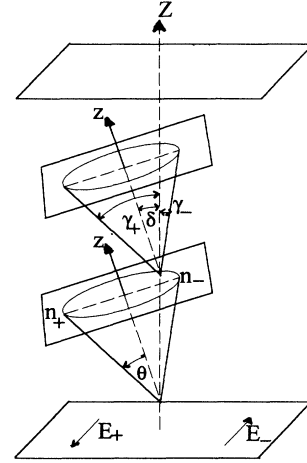


FIG. 4. Illustration of the director geometry associated with the unwinding of the helix in an applied electric field.  $\theta$  is the cone angle of the  $S_C^*$  phase and  $\delta$  the angle between the density wave normal and the cell wall.  $n_+$  and  $\gamma_+$  and  $n_-$  and  $\gamma_-$  are the unwound primary director and measured tilt angles for positive and negative fields, respectively.

The solution of this equation is just [17–19]

$$z(\phi) = \int_0^\phi \left[ C - 2 \frac{P_S}{B_3} E \cos \psi \right]^{-1/2} d\psi, \quad (3)$$

where, for a symmetrically twisted geometry in a thin cell with a thickness  $d$ , the constant  $C$  is obtained by minimizing the free energy in the whole cell, in a manner similar to that presented in [18],

$$\left. \left[ \frac{d\phi}{dz} \right] \right|_{\phi=\phi_B} = \left[ C - \frac{2P_S}{B_3} E \cos \phi_B \right]^{1/2} = q_0, \quad (4)$$

i.e.,

$$C = q_0^2 + \frac{2P_S}{B_3} E \cos \phi_B, \quad (5)$$

where  $\pm \phi_B$  are the director twist angles at the two surfaces of the cell, determined by the boundary condition

$$\int_{-\phi_B}^{\phi_B} \left[ C - \frac{2P_S}{B_3} E \cos \phi \right]^{-1/2} d\phi = d. \quad (6)$$

From the above equations we see that if the helical pitch  $p_0$  is determined from experiment, then the field dependence of the twist angle profile through the cell will yield the unknown parameter  $P_S/B_3$ . If, in addition, we know  $P_S$ , in this case supplied by the manufacturer of the liquid crystal, then  $B_3$  is determined. Thus, all we have to do is to obtain angle dependent reflectivities for a thin cell as a function of in-plane voltage and to fit the data obtained to modeling theory to give  $\theta$  and  $\phi(z)$ ; we thereby obtain the cone angle, the helical pitch  $p_0$ , and the twist elastic constant  $B_3$ .

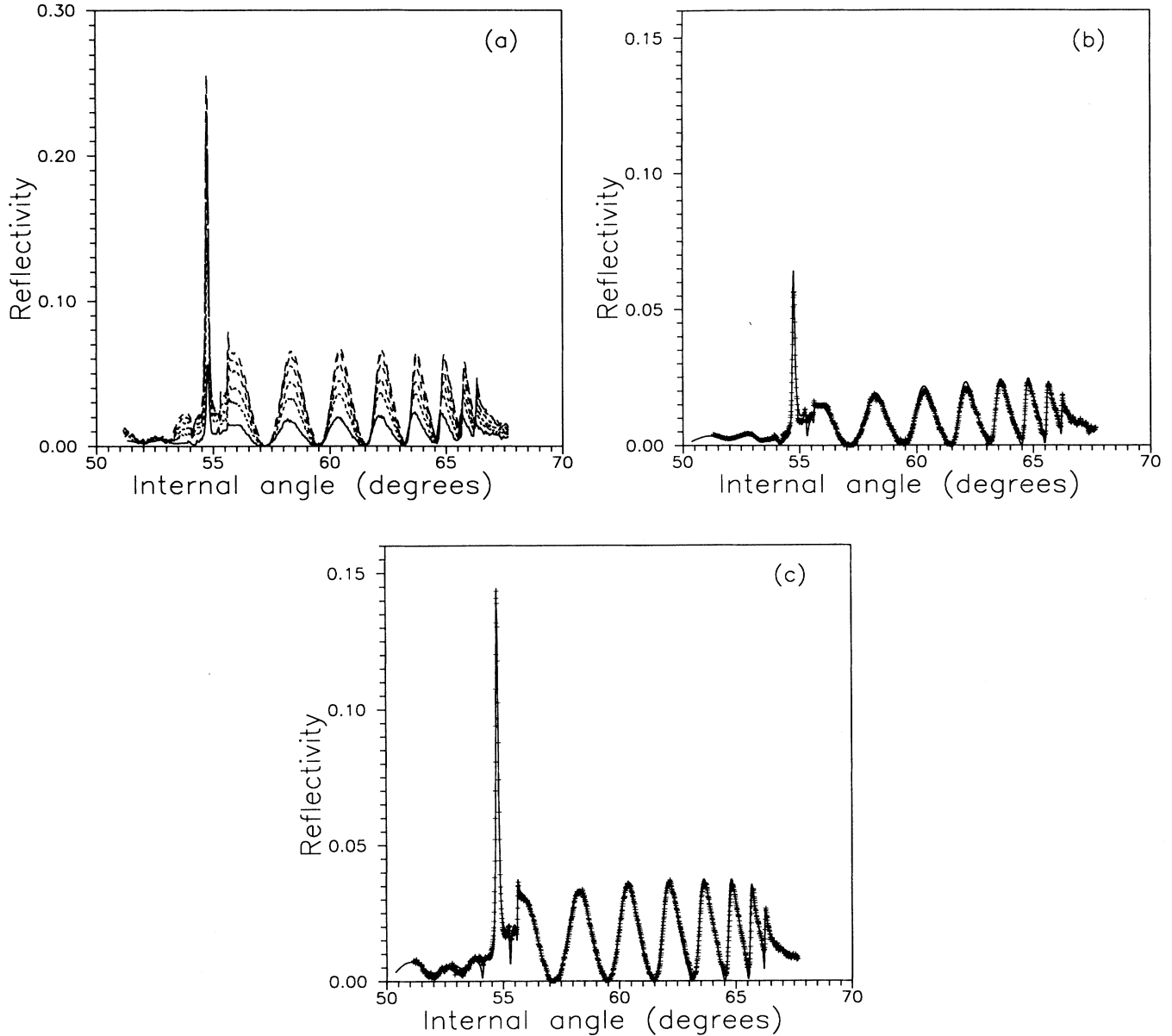


FIG. 5. (a) Experimental data for the  $s$  to  $p$  conversion reflectivity  $R_{sp}$  for different applied dc electric fields: The solid line is for zero field and the dotted lines are for external applied voltages from 10 to 50 V in steps of 10 V. The signal is seen to increase with increasing applied voltage; (b) and (c) show the theoretical fit to the  $R_{sp}$  data for 0 and 10 V applied, respectively.

### III. EXPERIMENTS

The sample geometry used is illustrated in Fig. 2. A high index ( $n = 1.800$  at 632.8 nm) glass prism and a low index ( $n = 1.457$  at 632.8 nm) glass substrate are separated with  $3.5 \mu\text{m}$  Mylar spacers. Both of the inner glass surfaces are uncoated except for the two 200 nm thick silver electrodes deposited by thermal evaporation onto the substrate, having a 3 mm gap between them. The parallel inner edges of these two electrodes are orthogonal to the plane of incidence, the radiation from a HeNe laser being arranged to arrive at the center of the elec-

trode gap. In order to fill the cell, it is placed in a temperature controlled environment with stability of temperature control of  $\pm 0.05^\circ\text{C}$  and heated to  $100^\circ\text{C}$ . At this temperature it is capillary filled with a SCE 13 (Merck). Once filled, the temperature is reduced quite rapidly (a few degrees per hour) to a temperature just higher than the  $S_C^*$  to  $S_A$  phase transition. Next, with a dc potential of 1.5 kV applied between the two silver electrodes, the sample is cooled at about  $0.5^\circ\text{C}$  per hour into the  $S_C^*$  phase. This produces a monodomain of homeotropically aligned material, with the helicity unwound, in almost all of the cell except very near the surfaces, where a small

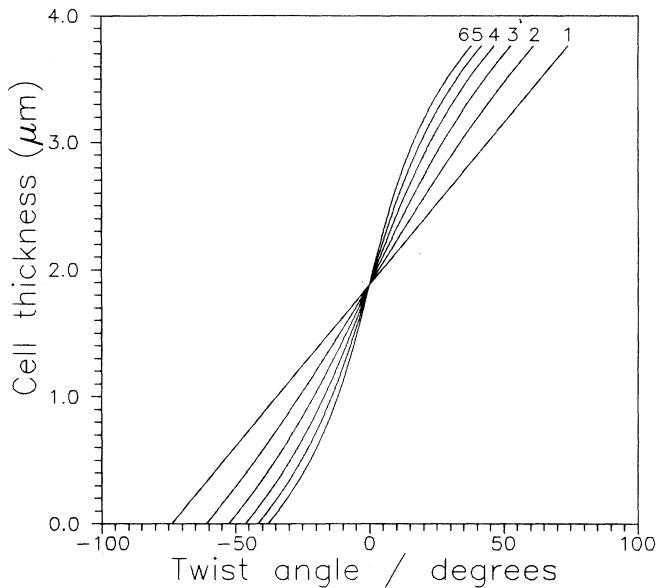


FIG. 6. Calculated twist angle profile through the cell for the best fit to experimental data shown in Fig. 5(a). Curves 1–6 correspond to the 0, 10, 20, 30, 40, and 50 V cases, respectively.

twist occurs. Once the monodomain has formed (this is established by examining the angular dependent  $s$  to  $p$  conversion reflectivity from the cell), the voltage is slowly reduced to zero, with data being acquired as the helix progressively rewinds itself. The voltage is then reapplied by slowly increasing it; further slow cooling is allowed, and data are taken at other temperatures.

In order to establish the quality of the monodomain and to record the angular dependent reflectivity data at many temperatures and voltages, the complete cell in its oven is placed on a computer controlled rotating table. The appropriate set of angle dependent reflectivity ( $R_{sp}$ ) data are recorded as reported elsewhere [15,16].

Because the gap of 3 mm between the electrodes is greater than the probe beam diameter, of the order of 1 mm, careful positioning of the probe beam in the center of the gap means that the area of liquid crystal studied is not influenced by boundary constraints at the silver electrodes. By careful fitting of modeled reflectivity curves produced from a scattering matrix multilayer optics program, the full optical tensor profile throughout the cell is established for all temperatures and voltages.

#### IV. RESULTS AND DISCUSSION

Initially, results were taken with the cell at 52.5°C. This is some 3.31°C lower than the  $S_C^*$  to  $S_A$  phase transition temperature of 55.81°C recorded for this cell by observing the electroclinic effect [14]. Two sets of fitted reflectivity data in the  $S_C^*$  phase are shown in Fig. 3. The data (crosses) are fitted by the theoretical prediction (solid line) based on a model of a simple tilted uniaxial slab with very thin (<40 nm) surface regions, over which there is a small director twist, and with the direc-

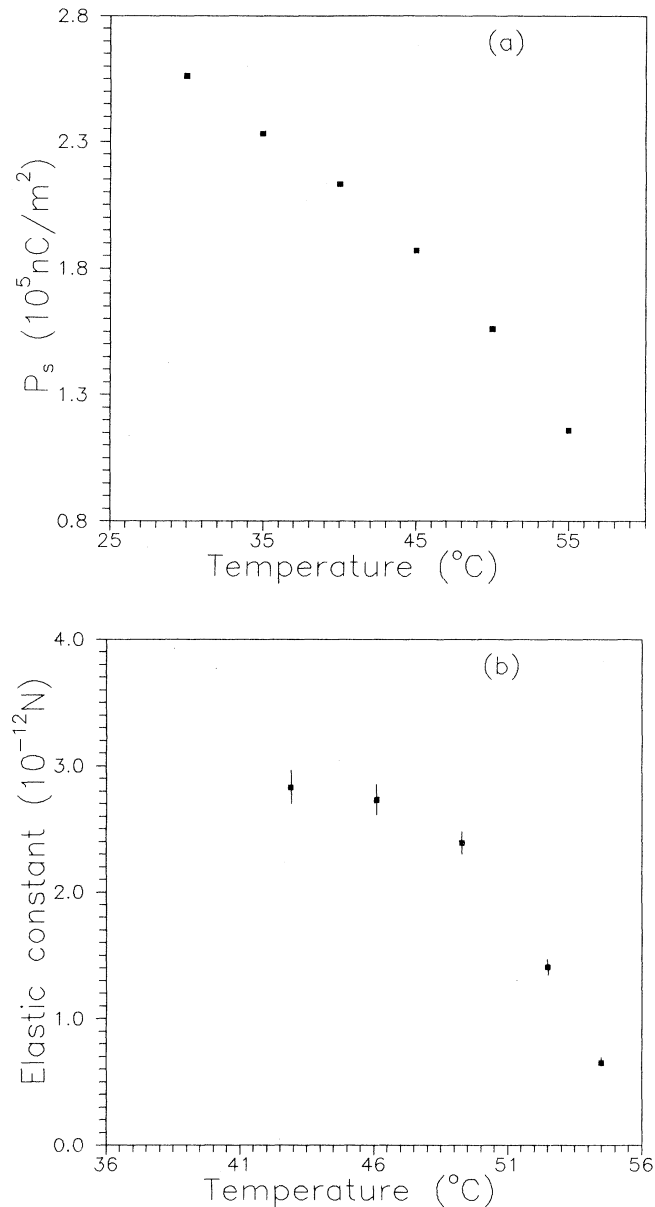


FIG. 7. (a) Variation of the spontaneous polarization with temperature as measured by Merck. (b) Variation of the twist elastic constant with temperature in the region of the  $S_C^*$  to  $S_A$  phase transition.

tor tilt assumed to vary linearly from the bulk tilt to the surface normal. These two data sets were taken with applied potentials of 1.5 and  $-1.5$  kV between the two electrodes. The fact that the signal levels are different for the two data sets is due to the  $S_C^*$  density wave normal being at a slight angle to the cell normal, as illustrated in Fig. 4. With a density wave normal tilt of  $\delta$ , the two fitted total tilt angles of the bulk of the cell are  $\gamma_+ (= \theta + \delta)$  and  $\gamma_- (= -\theta + \delta)$ , where  $\theta$  is the cone angle at the temperature of observation. At 52.5°C we determine  $\theta = (\gamma_+ + \gamma_-)/2 = 9.65^\circ$  and  $\delta = (\gamma_+ - \gamma_-)/2$

$= 1.75^\circ$ . A point to note is that while there is evidence of optical biaxiality from a homogeneously aligned cell [16] of FLC, here for a homeotropic alignment the influence of optical biaxiality is negligible and a simple uniaxial model adequately predicts the optical response of the cell for the geometry used. From such model predictions the cell thickness is found to be  $d = 3.765 \mu\text{m}$ , while at  $52.5^\circ\text{C}$   $\epsilon_{\parallel} = 2.7242 + i0.0003$  and  $\epsilon_{\perp} = 2.2125 + i0.0004$ .

The very obvious fact, from Fig. 3, that the uniform uniaxial tilted slab in almost the whole cell gives such an excellent fit to the data shows clearly that the  $S_C^*$  helix is unwound except very near the surfaces and that there is a monodomain in the cell. Continued reduction of the applied voltage with reflectivity data taken at regular voltage intervals gives the data shown in Fig. 5(a). It is very clear that as the applied field is reduced, the  $s$  to  $p$  conversion signal weakens. This reflects the fact that the helix is progressively winding up and a lower proportion of the cell's director lies tilted out of the plane of incidence. These data are a little more difficult to fit since the FLC is no longer a uniform slab. Now it is twisted in a manner that depends on the voltage, the twist rate across the cell varying with position in the cell. If we guess the parameter  $P_S/B_3$  in Eqs. (3)–(6), it allows us to predict the dependence of  $\phi$  on  $z$ , provided we know the natural helical pitch  $p_0$ . This is readily determined by fitting the data taken at zero volts [see Fig. 5(b)], using the already obtained  $\epsilon_{\parallel}$ ,  $\epsilon_{\perp}$ ,  $\theta$ ,  $\delta$ , and  $d$  from fits at 1.5 kV. At  $52.5^\circ\text{C}$  this gives a total helical winding across the cell of  $-74^\circ$  at one surface to  $+74^\circ$  at the other—a total twist of  $148^\circ$ . Thus from our knowledge of  $d = 3.765 \mu\text{m}$ , we have  $p_0 = 9.16 \mu\text{m}$ . Now all we have to do for the finite  $E$  field data is to adjust  $P_S/B_3$  in Eqs. (3)–(6) until the modeling of the optical response of the FLC cell fits the recorded data.

Figure 5(c) shows a fit of data at 10 V and  $52.5^\circ\text{C}$  corresponding to the twist profile shown in Fig. 6(a) (curve 2) with the parameter  $P_S/B_3 = 9.83 \times 10^7 \text{ C/m}^2 \text{ N}$ . Note that in evaluating Eqs. (3)–(6) we have taken the electric field at the center of the cell to be that of an infinitely long strip electrode system—for which  $E = 2V/\pi W$  [8], where  $V$  is the applied voltage and  $W$  the electrode gap width. Sets of data at different voltages of the type shown in Fig. 5(a) are fitted with the twist distributions shown in Fig. 6. These fits give constant values for  $P_S/B_3$  at each applied field. Using a value for the spontaneous polarization of  $P_S = 1.35 \times 10^5 \text{ nC/m}^2$  [its variation with temperature is shown in Fig. 7(a)] obtained from the chemical suppliers Merck, we then calculate the values of  $B_3$  for different applied voltages, obtaining the average value of  $B_3 = 1.41 \times 10^{-12} \text{ N}$  for SCE 13 at  $52.5^\circ\text{C}$ .

Using this same procedure for high quality data relatively close to the  $S_C^*$  to  $S_A$  phase transition, we get the temperature dependence of  $B_3$  shown in Fig. 7(b). (For lower temperatures there is a tendency for the cell to lose its monodomain character, particularly at low applied fields, making it very difficult to obtain and fit data and thus to determine  $B_3$  with any confidence.) The uncertainty in  $B_3$  of  $\pm 5\%$  is estimated from our knowledge of

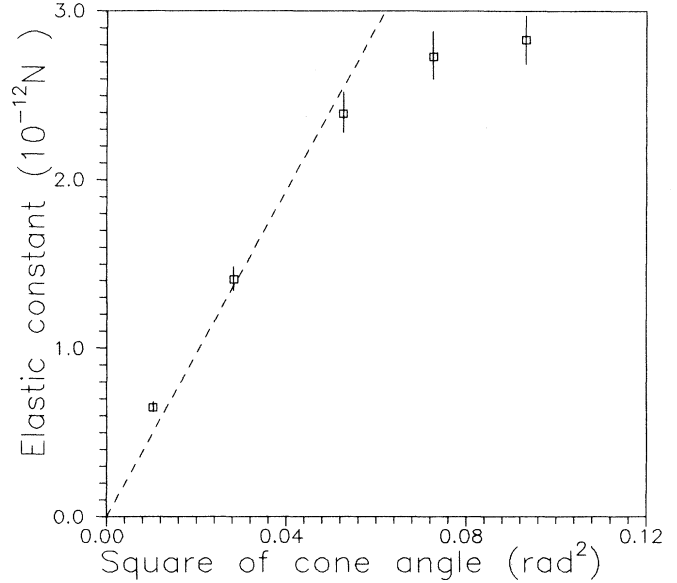


FIG. 8. Graph showing the variation of  $B_3$  with the square of the cone angle.

the range of the azimuthal angle  $\phi$ , which is determined to  $\pm 0.5^\circ$ . We have included no estimate of error in  $B_3$  due to the uncertainty in  $P_S$ , which is unknown. Thus our given error reflects the uncertainty in our own measurement, more correctly that of the parameter  $P_S/B_3$ .

From mean-field theory  $B_3$  is expected to vary as  $B_3 \propto \theta^2$  [20]. A plot of this form for our data for  $B_3$  against the square of the cone angle [14], Fig. 8, shows that the simple relationship appears true close to the phase transition but that the magnitude of  $B_3$  rises less rapidly than expected as the temperature is decreased, in accord with other experimental results [7].

## V. CONCLUSIONS

In this study the optical excitation of a series of half-leaky guided modes has been used to characterize in detail the optical tensor profile in a homeotropically aligned ferroelectric liquid crystal (SCE 13) layer. Uniform homeotropic alignment is realized, with no surface aligning layer, by the application of an in-plane dc field, which unwinds the helix in the  $S_C^*$  phase, producing a perfect monodomain. By slowly reducing the applied field, the FLC helix progressively forms with the monodomain maintained, at least for temperatures within about  $15^\circ\text{C}$  of the  $S_C^*$  to  $S_A$  phase transition temperature. By theoretical fitting of the experimentally recorded data to predictions from models of the director profile in the cell both with and without applied fields, the ratio  $P_S/B_3$  may be obtained. Then with the manufacturer's values provided for  $P_S$ ,  $B_3$  is deduced. Values of  $B_3$  are thereby obtained at different temperatures, which, when compared with the previously determined cone angles, show

reasonable agreement with mean-field theory close to the phase transition, with deviations becoming significant for temperatures some 10°C away. Because there is very weak surface anchoring in the cell, it is believed that these values represent those for the “free” material.

#### ACKNOWLEDGMENTS

The authors appreciate the support of DRA (Malvern) and the Engineering and Physical Sciences Research Council for this study.

- 
- [1] R. B. Meyer, L. Liebert, L. Strzelecki, and P. Keller, *J. Phys. (Paris)* **36**, L69 (1975).
  - [2] C. Rosenblatt, R. Pindak, N. A. Clark, and R. B. Meyer, *Phys. Rev. Lett.* **42**, 1220 (1979).
  - [3] C. Rosenblatt, R. B. Meyer, R. Pindak, and M. A. Clark, *Phys. Rev. A* **21**, 140 (1980).
  - [4] W. Kuczynski, S. T. Lagerwall, and B. Stebler, *Proceedings of the Eleventh International Liquid Crystal Conference*, edited by J. D. Litsker (University of California, Berkeley, 1986).
  - [5] K. Kondo, T. Kitamura, and A. Mukoh, *Proceedings of the Twelfth International Liquid Crystal Conference*, edited by H. Stegemeyer and F. Schneider, (University of Freiburg, Freiburg, 1988).
  - [6] M. Kawaida, M. Nakagawa, and T. Akahane, *Liq. Cryst.* **5**, 1115 (1989).
  - [7] M. Kawaida and T. Akahane, *Jpn. J. Appl. Phys.* **29**, 340 (1990).
  - [8] M. H. Lu, K. A. Crandall, and C. Rosenblatt, *Phys. Rev. Lett.* **68**, 3575 (1992).
  - [9] N. A. Clark and S. T. Lagerwall, *Appl. Phys. Lett.* **36**, 899 (1980).
  - [10] M. Kawaida and T. Akahane, *Jpn. J. Appl. Phys.* **27**, L1365 (1988).
  - [11] H. Takezoe, K. Kondo, A. Fukuda, and E. Kuze, *Jpn. J. Appl. Phys.* **21**, L627 (1982).
  - [12] S. A. Rozanski, *Phys. Status Solidi A* **79**, 309 (1983).
  - [13] I. Abdulhalim, L. Benguigui, and R. Weil, *J. Phys. (Paris)* **46**, 1429 (1985).
  - [14] Fuzi Yang, G. W. Bradberry, and J. R. Sambles, *Phys. Rev. E* **50**, 2834 (1994).
  - [15] Fuzi Yang and J. R. Sambles, *J. Opt. Soc. Am. B* **10**, 858 (1993).
  - [16] Fuzi Yang and J. R. Sambles, *Liq. Cryst.* **13**, 1 (1993).
  - [17] R. B. Meyer, *Mol. Cryst. Liq. Cryst.* **40**, 33 (1977).
  - [18] V. E. Dmitrienko and V. A. Belyakov, *Zh. Eksp. Teor. Fiz.* **78**, 1568 (1980) [*Sov. Phys. JETP* **51**, 787 (1980)].
  - [19] Ph. Martinot-Lagarde, *Mol. Cryst. Liq. Cryst.* **66**, 61 (1981).
  - [20] Ph. Martinot-Lagarde, R. Duke, and G. Durand, *Mol. Cryst. Liq. Cryst.* **75**, 249 (1981).